Global Blue Economy

The blue economy is an economic arena that depends on the benefits and values realized from the coastal and marine environments. This book explains the 'sustainable blue economy' as a marine-based economy that provides social and economic benefits for current and future generations. It restores, protects, and maintains the diversity, productivity, and resilience of marine ecosystems, and is based on clean technologies, renewable energy, and circular material flows.

Features

- Illustrates the fundamental concepts, tools, techniques, and details of a global blue economy
- Describes the scale and scope of the global blue economy and the role that observations, measurements, and forecasts play in supporting the safe and effective use of the ocean and its resources
- Includes many case studies from different countries and explores energy demands with emphasis on offshore oil and gas exploration methods and techniques
- Stimulates the political will and actions of governments and other partners for activities that effectively shape the framework of blue economy developments in many countries
- Clarifies the links among blue economy, sustainable development, and economic growth, and recognizes the importance of sustainable development goals for enhancing the economic benefits from the sustainable uses of marine resources
- Investigates the problems that threaten marine ecosystems and presents a set of management toolboxes and models for solving the issues of the blue economy in selected countries

This book provides a survey of the current state of understanding, activities, and policies related to the blue economy as it is being pursued in different industries and countries. A comprehensive resource for anyone interested.

Applied Ecology and Environmental Management – A Series
*Series Editor: **Steven M. Bartell**, Oak Ridge Associated Universities;*
***Sven E. Jorgensen**, Copenhagen University, Denmark*

Global Blue Economy: Analysis, Developments, and Challenges
Md. Nazrul Islam and Steven M. Bartell

Managing Environmental Data: Principles, Techniques, and Best Practices
Gerald A. Burnette

Environmental Management Handbook, Second Edition – Six Volume Set, Second Edition
Edited by Brian D. Fath, Sven Erik Jorgensen

Sustainable Development Indicators: An Exergy-Based Approach
Søren Nors Nielsen

Environmental Management of Marine Ecosystems
Edited by Md. Nazrul Islam, Sven Erik Jorgensen

Ecotoxicology and Chemistry Applications in Environmental Management
Sven Erik Jorgensen

Ecological Forest Management Handbook
Edited by Guy R. Larocque

Integrated Environmental Management: A Transdisciplinary Approach
Sven Erik Jørgensen, Joao Carlos Marques, Søren Nors Nielsen

Ecological Processes Handbook
Luca Palmeri, Alberto Barausse, Sven Erik Jorgensen

Handbook of Inland Aquatic Ecosystem Management
Sven Erik Jorgensen, Jose Galizia Tundisi, Takako Matsumura Tundisi

Eco-Cities: A Planning Guide
Edited by Zhifeng Yang

For more information on this series, please visit: www.routledge.com/Applied-Ecology-and-Environmental-Management/book-series/CRCAPPECOENV?pd=published,forthcoming&pg=2&pp=12&so=pub&view=list

Global Blue Economy

Analysis, Developments, and Challenges

Edited by
Md. Nazrul Islam and Steven M. Bartell

CRC Press
Taylor & Francis Group
Boca Raton London New York

CRC Press is an imprint of the
Taylor & Francis Group, an **informa** business

First edition published 2023
by CRC Press
6000 Broken Sound Parkway NW, Suite 300, Boca Raton, FL 33487-2742

and by CRC Press
4 Park Square, Milton Park, Abingdon, Oxon, OX14 4RN

CRC Press is an imprint of Taylor & Francis Group, LLC

ISBN: 9781032012728 (hbk)
ISBN: 9781032026251 (pbk)
ISBN: 9781003184287 (ebk)

DOI: 10.1201/9781003184287

Typeset in Times
by Newgen Publishing UK

Dedication

To

SAHANAJ TAMANNA

(Wife of Prof. Dr. Md. Nazrul Islam)

&

SABABA MOBASHIRA ISLAM

(Daughter of Prof. Dr. Md. Nazrul Islam)

Contents

Preface..........xi
Acknowledgments..........xvii
About the Editors..........xix
List of Contributors..........xxi

Chapter 1 Concepts, Tools, and Pillars of the Blue Economy: A Synthesis and Critical Review..........1

Md. Nazrul Islam

Chapter 2 Realizing Blue Economy Potential in Malaysia, Opportunities and Challenges..........35

Hanizah Idris

Chapter 3 Optimizing the Connectivity of Salmon Farms: Role of Exposure to Wind, Tides, and Isolation..........61

Dmitry Aleynik, Thomas Adams, and Keith Davidson

Chapter 4 Offshore Fish Farming: Challenges and Developments in Fish Pen Designs..........87

Chien Ming Wang, Yunil Chu, Joerg Baumeister, Hong Zhang, Dong-Sheng Jeng, and Nagi Abdussamie

Chapter 5 Risk Finance for Natural Disaster in Lakes and Coastal Seas Using Modeling Techniques..........129

Jinxin Zhou, Kentaro Kikuchi, Hideya Kubo, Takero Yoshida, Md. Nazrul Islam, and Daisuke Kitazawa

Chapter 6 Blue Economy Prospects, Opportunities, Challenges, Risks, and Sustainable Development Pathways in Bangladesh..........147

Md. Simul Bhuyan, Md. Nazrul Islam, Mir Mohammad Ali, Md. Rashed-Un-Nabi, Md. Wahidul Alam, Monika Das, Ranjan Roy, Mohan Kumar Das, Istiak Ahamed Mojumder, and Sobnom Mustary

Chapter 7 Application of Blue Economy for Polymetallic Nodules from the Central Indian Ocean Basin..........195

Ankeeta A. Amonkar, Niyati Gopinath Kalangutkar, and Sridhar D. Iyer

Chapter 8 Development and Challenges of Indian Ocean Blue Economy and Opportunities for Sri Lanka ... 221

Nawalage S. Cooray, Upul Premarathna, Keerthi Sri Senarathna Atapaththu, and Tilak Priyadarshana

Chapter 9 Marine Ecosystem Services: SDGs Targets, Achievement and Linkages with a Blue Economy Perception ... 259

Md. Nazrul Islam, Sahanaj Tamanna, S. M. Rashedul Islam, and Md. Shahriar Islam

Chapter 10 The Blue Economy Paradigm and Seafloor Massive Sulfides along the Indian Ocean Ridge Systems ... 285

Niyati Gopinath Kalangutkar, Ankeeta A. Amonkar, and Sridhar D. Iyer

Chapter 11 Global Scenarios of Seaweed Cultivation: Science-Policy Nexus for Enhancing the Seaweeds and Algae Farming ... 309

Md. Nazrul Islam, Sahanaj Tamanna, Md. Shahriar Islam, and Md. Noman

Chapter 12 Deep-Sea Mining and Potential Risks, Opportunities, and Challenges ... 341

Nezha Mejjad and Marzia Rovere

Chapter 13 Modern Seafood Production to Enhance the Blue Economy: A Proposed Sustainable Model for Bangladesh ... 361

Md. Nazrul Islam, Sahanaj Tamanna, and Khaled Mahamud Khan

Chapter 14 New Challenges for Sustainable Plastic Recycling in Japan ... 395

Jeongsoo Yu, Shiori Osanai, Kosuke Toshiki, Xiaoyue Liu, Tadao Tanabe, Gaku Manago, Shuoyao Wang, Kevin Roy B. Serrona, Kazuaki Okubo, and Ryo Ikeda

Chapter 15 Marine Pollution and Ecosystem Health: Challenges for Developing Sustainable Blue Economy ... 413

Md. Nazrul Islam, Sahanaj Tamanna, and Al Rabby Siemens

Chapter 16 Seaweed Farming Potential in India: An Assessment and Review ... 449

Muthuswamy Jaikumar, Ramadoss Dineshram, Temjensangba Imchen, Sourav Mandal, and Kannan Rangesh

Chapter 17 Modeling of Marine Policy Regime Creation for Enhancing Blue Economy in Global to Regional Aspects 471

Md. Nazrul Islam

Index 501

10 The Blue Economy Paradigm and Seafloor Massive Sulfides along the Indian Ocean Ridge Systems

Niyati Gopinath Kalangutkar,[1] Ankeeta A. Amonkar,[2] and Sridhar D. Iyer[3]*
[1] School of Earth, Ocean and Atmospheric Science, Goa University, Taleigao Plateau, Goa, India
[2] Dnyanprassarak Mandal's College and Research Centre, Mapusa, Goa, India
[3] Formerly with CSIR-National Institute of Oceanography, Dona Paula, Goa, India
*Corresponding author: Niyati Gopinath Kalangutkar
E-mail: niyati@unigoa.ac.in; ankeetaamonkar9@gmail.com; sdiyer2001@gmail.com

CONTENTS

10.1 Introduction 285
10.2 Hydrothermal Mineralization and Morpho-Tectonic Controls 287
10.3 Morpho-Tectonics and Hydrothermal Sites of the IORS 287
10.3.1 The Carlsberg Ridge (CR) 292
10.3.2 Central Indian Ridge (CIR) 293
10.3.3 South-East Indian Ridge (SEIR) 295
10.3.4 South-West Indian Ridge (SWIR) 295
10.4 The Blue Economy of Seafloor Massive Sulfides 297
10.4.1 Exploration 297
10.4.2 Environment 298
10.4.3 Exploitation 299
10.4.4 Enrichment 300
10.4.5 Economics 300
10.5 Conclusion 301
Acknowledgements 302
References 302

10.1 INTRODUCTION

The 70,000 km long global system of mid-ocean ridges (MOR) manifest in the Indian Ocean as four major ridge systems which are collectively called, the Indian Ocean Ridge System (IORS). The ridge systems are the Carlsberg Ridge (CR) which trends in an NW direction and protrudes into the Red Sea through the Gulf of Aden. The CR snakes towards the equator to form the Central Indian

DOI: 10.1201/9781003184287-10

Ridge (CIR) which bifurcates at the Rodriguez Triple Junction (RTJ, 25°S, 70°E) into the South West Indian Ridge (SWIR) and the South East Indian Ridge (SEIR) (Iyer and Ray, 2003). This inverted 'Y' IORS is less investigated relative to the Mid-Atlantic Ridge (MAR) which is also a slow to medium spreading ridge and has a comparable geology and tectonic architecture. Yet, the MAR has tens of hydrothermal vent sites of variable dimensions with abundant seafloor massive sulfides (SMS), also known as the volcanogenic massive sulfides (VMS) that are hosted by lava flow, basalt outcrops and serpentinites.

The IORS was believed to be less favourable for hydrothermal metallogenesis until the discovery of hot brine and metalliferous sediments in the Red Sea (Degens and Ross, 1969). In the Indian Ocean, a number of low and high intensity hydrothermal sites have been reported. Among the low intensity sites are some segments along the CR, regions near the Vityaz fracture zone and areas between latitudes 24° and 37°S and longitudes 49° and 60°E; and along the SEIR. Under the bilateral India-Germany collaborative programme *GEMINO*, several low intensity sites were found (Herzig and Plüger, 1988). A few high intensity sites such as the Red Sea spreading centre, the Sonne hydrothermal plume site (24°00.3'S and 69°39.6'E) and Geodyn plume site (19°29'S, 65°44'E) were located. The seafloor at the slow spreading Red Sea rift, representing an early stage in the opening of an ocean basin, contains one of the largest deep sea mineral deposits. The Atlantis II Deep (21°24'N and 38°03'E) is the most significant active hydrothermal site in the Red Sea, consisting of a stratified pool of high temperature (~ 56°C) brine, about 10 times more saline than the seawater. The metalliferous sediments have high concentrations of zinc (Zn 1.7%), copper (Cu 0.43%), silver (Ag 0.18%), and cobalt (Co 0.14%). The best estimate suggests that Atlantis II Deep deposits contain about 200 million tones (mt) of ore, including 3.2 mt of Zn and 0.8 mt of Cu (Swallow and Crease, 1965; Scholten et al. 2000).

The United Nations Convention on the Law of the Sea (UNCLOS) proposed a detailed legal framework for rights and obligations of countries to access, use and reclaim marine resources from territorial waters and open oceans. The UNCLOS document (Article 76) was signed on 10th Dec 1982 in Jamaica and implemented on 16 Nov 1994. The ocean space under the jurisdiction of a country can be classified into several maritime zones. A coastal nation has full rights over resources that can be derived from the air, the water column, the seabed, and sub-surface from its respective coastal waters (5.55 km into the sea from the coast), its territorial sea (5.55 to 22.2 km) and its contiguous zone (22.4 to 44.4 km). A nation can access resources from the water column, seabed and sub-surface that occur within its Exclusive Economic Zone (EEZ) (44.4 to 370 km), while resources only from the seabed and sub-surface strata can be exploited from the Extended Continental Shelf (ECS/CS) 370 to 647.5 km).

The global coasts and oceans are repositories of placer minerals (coastal and nearshore), phosphorites, fossil fuels (oil, gas, methane), SMS along the MOR, cobalt-rich crusts over seamounts and polymetallic manganese nodules in the abyssal depth. The exploration, mining and allied activities for these resources can be sustainably carried out by applying the various features of the blue economy (Mukhopadhyay et al. 2020).

The United Nations Conference on Sustainable Development (UNCSD) at the Rio+20 Conference (Rio de Janeiro, June 20–22, 2012) emphasized the concept of the 'Blue Economy' (BE) as it pertains to oceans and seas. The major sectors of the BE are food security, harnessing energy-minerals-pharma products, climate change, increasing trade and investments, improving maritime activities, tourism (leisure, recreation), employment opportunities, and socio-economic growth (Pauli, 2010). It has been suggested that the BE could support sustained fiscal growth, enhance social integration, and improve human welfare (UNCSD, 2018). During exploration and exploitation of marine minerals there are opportunities to develop and utilize innovative technology and further, there would be ample scope for skilled and unskilled workers, onboard and on land.

During the first IORA (Indian Ocean Rim Association) Blue Economy Dialogue that was held on 17th and 18th Aug 2015 in Goa (India) the sectors that were discussed were fisheries and aquaculture, renewable marine energy, accounting frameworks, ports, shipping and related activities, and explorations for marine minerals. The Dialogue was followed by the First Ministerial Blue Economy Conference (Mauritius, Sep 2–3 2015) and the Second Indian Ocean Dialogue (Perth, Australia, Sep 2015). In Mauritius, the Blue Economy Declaration was adopted and this sought to use ocean resources to boost a country's economy, create jobs, progress technologically, amongst others, while simultaneously protecting the environment *(www.iora.int)*. During the second ministerial BE conference (Indonesia, May 8–10 2017) the IORA Secretariat identified major sectors: Fisheries and Aquaculture; Renewable Ocean Energy; Seaports and Shipping; Minerals and Hydrocarbons; Tourism; Marine Biotechnology; and Research and Development.

The BE paradigm envisages mining resources in the above-mentioned maritime zones in best, efficient, responsible and workable ways. This is along the line of the UN's Sustainable Development Goal (SDG-14) that is concerned with conserving and a justifiable use of the oceans and seas. The resources available beyond the ECS are reserved for the common heritage of mankind, and cannot be mined by any country unless permitted by the UNCLOS (presently it is the International Seabed Authority, ISA based in Jamaica).

Deep sea minerals have been recognised as principal sources of base metals that are useful in high- and green-technology industries (Hein et al. 2013). In this chapter, firstly we synthesize the studies made of the IORS hydrothermal vents in terms of their geology, mineralogy, composition and other parametres. Secondly, this is followed by a discussion of the application of the BE to recover the SMS.

10.2 HYDROTHERMAL MINERALIZATION AND MORPHO-TECTONIC CONTROLS

According to Veizer et al. (1989) the modern seafloor hydrothermal ore deposits that are related to the mineralization of base metals reflect the ~100 Ma geological history of the Earth. Sea water-rock interaction leads to the leaching of metals and the sformation of hydrothermal convection systems in areas of rifting, subsidence and thinning of the crust. Initially, hot mafic-ultramafic magma acts as a heat source and initiates convective circulation of hydrothermal fluids that ascend within the serpentinized mantle peridotite and deposits SMS (Franklin et al. 2005; Garuti et al. 2008). The SMS is precipitated from the hot solution at ~600°C from aqueous solutions within the upper crust (Barnes and Rose, 1998). The congenial sites for a variety of mineral deposits are active magmatic arcs, continental margins, MOR, fore-arcs and back-arcs (Bierlein et al. 2009).

The formation and deposition of SMS are influenced by morpho-structural features such as MOR, fracture zones with deep roots into the upper mantle (Kutina, 1983), syn-volcanic structures, folds, faults, unconformities and shear zones, fault-bounded axial rifts, and seamount calderas adjacent to extensional structures submerged island arcs (Scott, 1992; Fouquet, 1997). Because these structures are the pathways for the ascending hydrothermal solution and control the geometry of the ore deposits, it is important to locate the economic mineral deposits through geological, geophysical, and geochemical approaches.

10.3 MORPHO-TECTONICS AND HYDROTHERMAL SITES OF THE IORS

We provide a gist of the studies of the work carried out along the IORS, by the international community and by India. Table 10.1 is a compilation of the hydrothermal areas that occur along the IORS while some of the hydrothermal sites are shown in Figure 10.1.

TABLE 10.1
Hydrothermal Vent Location and Work Carried out by Various Researchers

Sr no.	Name of the Site	Latitude	Longitude	Authors	Studies Carried out
			South West Indian Ridge		
	Western part	40°–60°S	10°–25°E	Suo et al. (2017)	Analysed spreading rate, bathymetry, gravity and geochemical data.
	Eastern part	20°–45°S	49°–70°E		
	–	37°47′S	49°39’E	Tao et al. (2011)	Mineralogy and geochemistry of sulfide chimneys.
	Segment 27	37°80’–37°50’S	50°80’–50°40’E	Yue et al. (2019)	Identified turbidity anomalies and oxidation reduction potential values.
	–	38°–38.4°S	48.1–48.7°E	Chen et al. (2021)	Bathymetry, normal faults, anomalous turbidity values and oxidation reduction potential.
	–	28°50′–26°50′S	63°–68°E	Agarwal et al. (2019)	Major, Trace and REE of RTJ and Mt Jourdanne samples.
	Tiancheng	27°51′S	63°55′E	Chen et al. (2018)	Discovered 2 hydrothermal fields.
	Tianzuo	27°57′S	63°32′E		
	Longqi field	37°47′S	49.6°E	Ji et al. (2017)	H_2, CH_4 and other chemical data of hydrothermal fluids.
	Longqi	37°47’S	49.6°E	Zhou et al. (2018)	Investigated biodiversity and biogeographical relationship.
	Tiancheng	27°51′S	63°55′E		
	Duanqiao	37°39′S	50°24′E		
	Kairei	25°S	70°E	Han et al. (2018)	Mineralogy and geochemistry of hydrothermal precipitates.
	Pelagia	26°S	71°E		16S rRNA tags from different sites were analysed and compared with other marine environments.
	• SWIR from 49°E to 53°E	38°S	49°E	Tao et al. (2014)	REE, XRD of pyrite, silica, opal and sulfide deposits.
	• Longqi	36°S	53°E		
	• 50°24’E hydrothermal field	37°47’S 37°39’S	49.6°E 50°24’E		
	• 50°56’E carbonate field	37°37’S	50°56’E		
	• SWIR 63° field	27°57’S	63°32’E		
	–	43°S	40°E	Ren et al. (2016)	Analysis of topographic, geology, geophysics and metallogenic data. Proposed a prospecting prediction model.
	Longqi	37°47’S	49.6°E	Wang et al. (2018)	He-Ar-S isotopes
	Tiancheng	27°51′S	63°55′E		
	Duanqiao	37°39′S	50°24′E		
	Yuhuang	36°–38°S	49°–52°E		
	Kairei	25°S	70°E		
	Edmond	23.8778°S	69.5973°E		

Different sites	27°–38°S	46°–63°E	Chen et al. (2021)	Geochemistry of surface sediments and hydrothermal deposits.
Yuhuang-1	36°–38°N	49°–52°E	Liao et al. (2019)	Zn isotope compositions, element ratios of Zn, Fe, Cu, and Cd in sulfides.
Yuhuang-1	36°–38°N	49°–52°E	Liao et al. (2019)	Major and trace elements, sulfur isotopes analysis.
Duanqiao	37°39′ S	50°24′ E	Zhu et al. (2020)	Elemental concentration and Hg isotope analysis.
Yuhuang	36°–38°S	49°–52°E		
–			Kalangutkar et al. (2021)	Hydrothermal signatures in FeMn from SWIR
Central Indian Ridge				
Onnuri Vent Field	8°10.1'S	68°08.2'E	Kim et al. (2020)	Plume sample, water column, fauna of vent samples.
Segment 2	9°47'S	66°41.9'E		
Segment 3	11°20'S	66°26'E		
Edmond vent field	23°52.68′S	69°35.80E	Wu et al. (2018)	Mineralogy and geochemistry of sphalerite to identify different textures and micro-environments.
A1A	20 ° 20'S	68 °E	Briais (1995)	Analysis of segments between 20° 30'S and 25° 30'S (Rodriguez Triple Junction).
A1B	26 °S	70 ° 30'E		
A2A	23°23.56'S	69°14.53E	Halbach et al. (1995)	Sonne Field – First SMS in the Indian Ocean.
Yokoniwa	25°16'S	70°05'E	Fujii and Okino (2018)	Magnetization of hydrothermally altered zone and host lava flows.
Kairei	25°21'S	70°03'E		
Solitaire field	19°33.410S	65°50.89'E	Kawagucci et al. (2016)	Fluid chemistry and microbial communities in chimney habitats.
Dodo hydrothermal field	18°20.190S	65°17.99'E		
Between 10°18'S and 10°57'S	10°47.5'S	66°38.6'E	Ray et al.(2020)	Analysis of dissolved Mn and He
Yokoniwa	25°16'S	70°04'E	Fujii et al.(2016)	Magnetic studies using an AUV and manned vehicle.
Dodo	18°20'S,	65°17E	Nakamura et al. (2012)	Measured chlorine, dissolved gases (H_2, CH_4, CO_2, and so forth.), pH, fauna and flora, rRNA gene sequencing was done.
Solitaire	19°33'S	65°50E		
A1A	20° 20'S	68°E	Briais (1995)	Bathymetry, fracture zones, tectonics.
A1B	26°S	70°30'E		
A2A	23°23.56'S	69°14.53'E	Halbach et al. (1995)	Massive sulfide mineralogy and chemistry.
MESO	23°23.56'S	69°14.53'E	Halbach et al. (1998)	Geology, mineral zonation, different sulfide types, stages of formation and decay of a modern SMS.
MESO	23°23.63'–38°3.38'S	69°14.43'–69°14.48'E	Halbach et al. (2002)	Hydrothermal sulfide impregnated and pure silica precipitates, sulfides chimney.

(*continued*)

TABLE 10.1 (Continued)
Hydrothermal Vent Location and Work Carried out by Various Researchers

Sr no.	Name of the Site	Latitude	Longitude	Authors	Studies Carried out
	MESO	23°23.56'S	69°14.53'E	Halbach and Münch (1997)	Study of sulfide chimneys.
	MESO	21.5°–23° S	68.5°–69.25° E	Herzig and Plüger (1988)	Mapping, photography, sampling to locate fossil/recent hydrothermal activity. Geochemistry of basalts, sediments, and water.
	MESO	27°–28°S	65°20'–66°40'E	Muller et al. (1999)	Variation of oceanic crustal thickness using seismic velocity model.
	MESO	23°23.63'S	69°14.43'E	Münch et al. (1999)	Hydrothermal mineralization, structural control, mineralogy, and geochemistry of sulfide chimneys.
	MESO	23°23.63' - 38°3.38'S	69°14.43' - 69°14.48'E	Lalou et al. (1998)	Radiochronological investigation of hydrothermal deposits.
	MESO	23°23.56'S	69°14.53'E	Plüger et al. (1990)	Geology
	–	23°52.68'S	69°35.80'E	Gallant and Von Damm (2006)	Chemical composition of hydrothermal fluids.
	–	23.88°S	69.60°E	Kumagai et al. (2008)	Geology and tectonics.
Carlsberg Ridge					
	Wocan	6°22'N	60°31'E	Wang et al. (2020)	Sulfur and iron isotope analysis.
	Wocan 1 Wocan 2	6°21'40'–6°21'50'N 6°22'30'–6°23'N	60°31'45'–60°31'30'E 60°30'45'–69°30'15E	Qiu et al. (2021)	Mineralogy, chemistry, Pb–Sr isotopes.
	Carlsberg ridge	3°42'–3°41.5'N	63°40'–63°50'E	Ray et al. (2012)	Temperature anomaly, oxidation-reduction potential, dissolved Mn and ^{3}He were analysed.
	Carlsberg Wocan-1 Wocan-2 Ridge flank Core sediments	6°21.796'N 6°21.866'N 6°35.675'N 4° 07.52'N	60°31.534'E 60°30.372'E 60°13.190'E 69°20.201'E	Popoola and Akintoye (2019)	Geochemistry of sediments and sulfides.

Tianxiu	3.67°N	63.83°E	Chen et al. (2020)	Precipitation of calcite veins in serpentinized, Carbon and Oxygen isotopes.
Wocan	6°22’N	60°31’E	Popoola et al. (2019)	Morphology, mineralogy and geochemistry of Fe-Si-Mn oxyhydroxides, sulfur isotopes.
Daxi	6°48′N	60°10′E	Wang et al. (2020)	Mineralogy, chemistry, and bathymetry studies.
Along ridge segment	10°N	66°E	Yu et al. (2016)	Major element and REE of 30 sediments from 24 sites.
Wocan	6°22’N	60°31’E	Wang et al. (2020)	Mineralogy and chemistry of Cu - rich chimneys and massive sulfides.

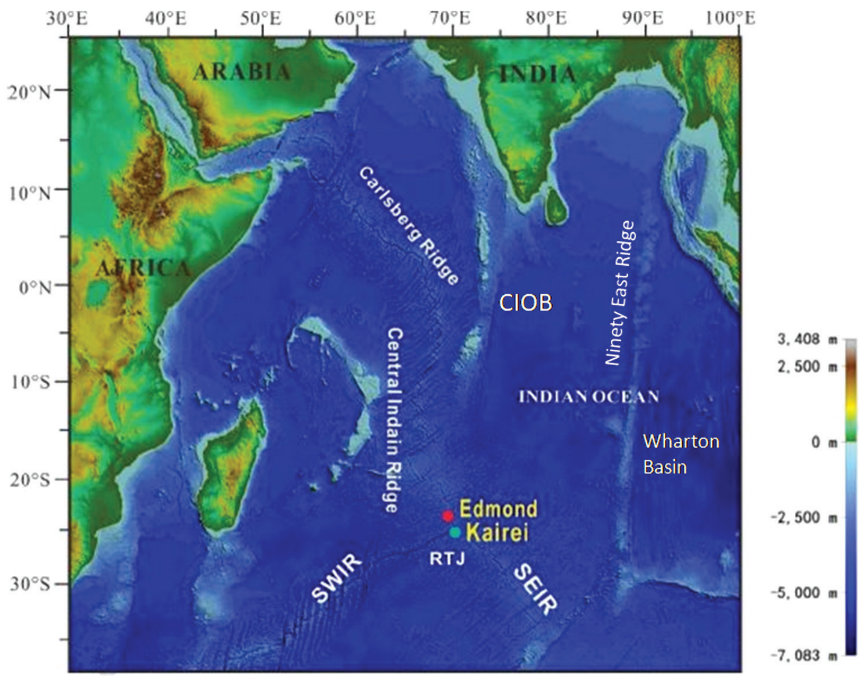

FIGURE 10.1 India's exploration area for SMS along the SWIR (Modified after https://isa.org.jm/index.php/map/government-india-0).

10.3.1 The Carlsberg Ridge (CR)

The Carlsberg Ridge is a slow spreading ridge with half-spreading rates between 11 and 16 mm/yr (henceforth half-rate will be used). The CR is devoid of major transform faults and is segmented by dextral, non-transform, and second-order discontinuities. Indications of weak hydrothermal activity were earlier detected in the CR (Kempe and Easton, 1974) and this was confirmed by iron-rich (28%) basal sediments from the DSDP Site 236 (1°40'S, 57°38'E) (Baturin and Rozanova, 1975).

During the maiden voyage in 1983 of *ORV Sagar Kanya* (India) from Germany to Goa, a segment of the CR was dredged and the basalts (Banerjee and Iyer, 1991; 1993; 2003; Iyer and Banerjee, 1993) and geophysical aspects were reported (Ramana et al. 1993). Subsequently, the ridge section between 2°30'S and 4°30'S and 62°30' to 66°15'E was mapped and basalts and upper mantle rocks were recovered (Mudholkar et al. 2002). Studies reported event plumes (Murton et al. 2006) and identification of hydrothermal activities along the various segments of the CR. Ray et al. (2012) reported hydrothermal plumes from unknown active vent(s) near 3°42′N/63°40E and 3°41.5′N/63°50′E. The magmatic/hydrothermal chalcopyrite, pyrite, and magnetite in the basalts at 3°37'S/64°07N (Banerjee and Iyer, 1993; 2003) are similar to sulfide - oxide minerals in the basalts at 5°23'N (Baturin and Rozanova, 1975).

During the 26th Chinese COMRA (China Ocean Mineral Resources Research and Development Association) a hydrothermal activity field with SMS was located along the CR at 3.5° - 3.8°N. Evidence for two separate vent fields were identified, one near 3°42′N, 63°40′E (Wocan) and another at 3°41.5′N, 63°50′E (Daxi). Prominent optical backscatter and thermal anomalies coupled with chemical (for example, helium ^{3}He, manganese Mn) signatures in seawater demonstrated the existence of hydrothermal sources on off-axis highs on the south wall of the CR. Although ultramafic rocks have been recovered near these sites, the light-scattering and dissolved Mn anomalies indicate that the plumes do not arise from a system driven solely by exothermic serpentinization (Ray et al. 2012). It was suggested that the source fluids for these two active sites may be a product of both ultramafic and basaltic/gabbroic fluid-rock interaction, similar to the Rainbow and Logatchev fields, MAR.

i) Wocan Hydrothermal Field: During the Chinese DY28th cruise along the CR in 2013, the basalt-hosted Wocan Hydrothermal Field (WHF) was found on the NW slope of an axial volcanic ridge at a water depth of ~3,000 m. The hydrothermal precipitates that were recovered were classified into four groups: (i) Cu-rich chimneys; (ii) Cu-rich massive sulfides; (iii) Fe-rich massive sulfides; and (iv) silicified massive sulfides (Wang et al. 2017). The mineralogy and geochemistry of metalliferous sediment were studied at the Wocan hydrothermal field active site (Wocan-1) and an inactive site (Wocan-2). Based on the mineralogy and morphology of sulfide and non-sulfide grains, bulk composition, and sulfur isotopes it was concluded that at Wocan-1 there is an intermediate - high temperature hydrothermal discharge; while Wocan-2 shows a moderate - extensive oxidation and secondary alterations by seawater in a low - intermediate environment (Popoola et al. 2019).

ii) The Daxi Vent Field: The Daxi Vent Field (DVF) is a basalt-hosted hydrothermal field located on a rifted volcanic ridge along a non-transform offset between two second-order ridge segments. At the DVF there are three hydrothermal sites, namely Central mound, NE mound, and South mound. Eight black smokers were observed in the Central mound which hosts the largest sulfide chimney 'Baochu Pagoda' of ~24 m height. Another inactive silica-rich chimney was observed in the NE mound. The sulfide chimneys are dominated by sphalerite and pyrrhotite with high Sn, Co and Ag; and silica-rich chimneys have high SiO_2 and Ba contents (Wang et al. 2020).

10.3.2 Central Indian Ridge (CIR)

The CIR with a half spreading rate of 20 - 30 mm/yr has structures, spreading kinematics and isotope geochemistry of erupted lava that are remarkably different from the other MOR (Drolia et al. 2003). Exploration related activities in the Indian Ocean commenced about four decades ago sometime in early 1983. The initial results were encouraging with the finding of characteristics He and Mn anomalies that indicated hydrothermal plume activities along segments of the CIR (Herzig and Plüger, 1988). The discovery of two fossil hydrothermal vent fields, the Sonne Field, and Mount Jourdanne Field, led to several new exploration programs in this region (Halbach et al. 1998; Munch et al. 2001). These were followed by the detection of the active hydrothermal fields, Kairei, and Edmond, where the first direct observations were made of active hydrothermal discharge, vent biota, and shimmering water (Hashimoto et al. 2001; Gamo et al. 2001; Van Dover et al. 2001). Some details of the hydrothermal sites found along the CIR are provided below.

(i) Sonne: Herzig and Plüger (1988) and Plüger et al. (1990) respectively reported the existence of Sonne (an inactive hydrothermal field, named after the famous German research vessel *FS Sonne*), and a first indication of a hydrothermal plume site (24º00.3'S) along the CIR. The Sonne field at 23°23.6'S and ~200 km NW of the RTJ, consists of hydrothermally influenced basalts and sediments, layered FeMn precipitates, and blocks of massive sulfides. The Edmond and Kairei hydrothermal fields were first recognized in 1993 and reported by Gamo et al. (1996; 2001) and Hashimoto et al. (2001), whereas the Dodo and Solitaire hydrothermal fields were discovered later (Nakamura et al. 2012).

(ii) Meso zone: The Meso zone is named after the *RV Met*eor and *RV Sonne* zone and is located at 23.3927°S and 69.2422°E. The Meso zone is at a distance of 270 km N of the RTJ on a neo-volcanic intra-rift ridge and covers an area of ~0.6 km². Three sites were identified with evidence of hydrothermal activity (Halbach et al. 1998). The sites are the Talus-Tips-Site (TTS) in the northern part, the Sonne Field (SF) in the central part and the Smooth Ground (SG) in the southern part of the mineralized zone *(www.interridge.org).* Hydrothermal mineralization and structural control in the Meso zone region were detailed by Munch et al. (1999) and sulfide-impregnated and pure silica precipitates of hydrothermal origin were reported by Halbach et al. (2002).

(iii) Kairei and Edmond: The Kairei and Edmond hydrothermal fields are located ~6 km to the east of the spreading axis on the eastern wall of the axial valley (Wilson, 1993). The Kairei field is developed on shoulder of the west-facing slope of the abyssal hill of CIR-1 (Hakuho Knoll) with flat or lobate lava flows, whereas the Edmond field has flat, partly wrinkled lava flows. Kairei field is along a linear ridge which is perhaps an abandoned ridge axis formed during ridge jump and has dunite and troctolite and a regional seafloor morphology that is distinctly heterogeneous within 30 km of the current ridge axis while regular ridge-parallel abyssal hills occur along the Edmond field (Kumagai et al. 2008; Van Dover et al. 2001). Both the fields have large and complex chimney structures with large massive sulfide mounds at their bases (Nakamura et al. 2012). But the morphological contrast between the two fields might have influenced the pathway of the recharged vent fluid, as evident from the composition of the fluids (Gallant and Von Damm, 2006).

Copper-rich chimney edifices and fragments rich in chalcopyrite, with pyrite, marcasite, wurtzite, and sphalerite occur in Kairei. Granular chalcopyrite decreases in amount and grain size towards the outer parts of the chimneys, while disseminated sphalerite and pyrite increase in the outer parts. This fact indicates a fall in temperatures towards the outer parts of the chimney. Active chimneys are nearly fresh and weathered products are present on the outer wall in contact with seawater or in inactive vents (Han et al. 2018). At the Edmond site are native Cu and Cu-sulfides (covellite, digenite and chalcocite), altered chalcopyrite, and outer walls have plentiful abundant sub-microscopic Au-Ag alloys (Wu et al. 2018).

(iv) Dodo and Solitaire: The Dodo hydrothermal field with active vents (18°20.1′S, 65°17.9′E; water depth 2,745 m) is located in the Dodo Great Lava Plain on the spreading axis of CIR segment 16 (Nakamura et al. 2012). The hydrothermal field is 10 km with smooth sheet flow lavas along the axis that indicate high production rates of basaltic melt, a feature similar to the East Pacific Rise (EPR). Potsunen, Tsukushi-1, and Tsukushi-2 are the three main chimneys. Black smoker discharges occur at Tsukushi-1 whereas, active chimneys and several inactive chimneys are near Tsukushi-2 (Nakamura et al. 2012). Extensive plume surveys using vertical and tow-yo hydrocasts and an autonomous underwater vehicle (AUV) led to identify anomalous concentrations of methane (CH_4), Mn, and ^3He (Kawagucci et al. 2008).

The Solitaire field (19°33.413'S, 65°50.888'E; at a depth of 2,606 m) is located on the Roger Plateau on the western ridge flank of CIR segment 15. Plume signatures of hydrothermally derived CH_4, Mn and ^3He abundance and a light transmission signal anomaly were evident (Kawagucci et al. 2008). In this field, three major chimney sites (Toukon-3, Tenkoji, and Liger) were identified with chimneys <5 m in height. At the Toukon-3 chimneys the emissions are clear fluids and a few black smoker discharges (Nakamura et al. 2012).

(v) OCC 1-1, OCC 2-1, OCC 3-1, OCC-3-2, OCC-4-1, and OCC-4-2: Strong hydrothermal plume signals were measured over the Oceanic Core Complexes (OCCs) along long-lived detachment faults that formed because of tectonic extension in the middle part of the CIR (8°S to 17°S) which has a morphology typical of slow spreading ridges (Pak et al. 2017; Kim et al. 2020). The OOCs are conduits for hydrothermal fluids which rise at off-axis regions. Pak et al. (2017) felt that the serpentinization and latent/cooling heat of the underlying mantle and magma supply heat for hydrothermal circulation, resulting in high-CH_3 concentration in the plumes. The Onnuri Vent Field (OVF) is located at the summit of OCC-3-2, and vents clear, low-temperature fluids, located on the ridge flanks of typical abyssal hill structures of a symmetrical ridge section. Hydrothermal mineralization is primarily silica-rich and disseminated sulfide with secondary Cu minerals, associated with hydrothermal precipitates (Kim et al. 2020)

India commenced the investigations of the CIR (initially funded by the Office of Naval Research and NSF, USA and later by the Indian government under the InRidge programme) and undertook studies between 3˚S and 11˚S, and between 66˚E and 69˚E. The areas included the transform faults (TF) Sealark, Vityaz, and Vema and the intervening ridge segments (Drolia et al. 2003). Later the morphotectonic features and petrological variations between 20°30′S and 23°07′S were detailed

(Mukhopadhyay et al. 2015). The possibility of hydrothermal activity in certain segments of the CIR was postulated by Banerjee and Ray (2013, 2015 and references therein). The magmatic and tectonic processes that resulted because of the interaction between the Reunion plume and CIR at the Vema Trench and along the Vema Fracture Zone was detailed (Dhawaskar et al. 2020). The InRidge programme also included studies of the CR and Andaman Back Arc Basin (ABAB) which are separately discussed.

10.3.3 South-East Indian Ridge (SEIR)

The SEIR is an intermediate spreading (30–35 mm/yr) and this is the fastest spreading rate of all the IORS (DeMets et al. 1990).

(i) Antarctic Australian Ridge (AAR): The AAR with a series of ridge segments and transform faults extending from 140°E to 180°E, has an intermediate spreading (~39-30 mm/yr) and its axial depth is relatively shallow (~2,200 m) (Choi et al. 2013). The KR1 and KR2 are first-order segments and bounded by transform faults. Hydrothermal activity has been noted at two first-order segments of the AAR: KR1 and KR2. Optical and oxidation-reduction-potential anomalies indicate multiple active sites on both segments (Hahm et al. 2015).

The KR1 segment (139.5°E, 122°W) shows large variations in its axial morphology that point to a variable magma supply. Alkalic to tholeiitic magmatism along KR1 may be potential source materials for alkaline basalts and are considered to be ancient, recycled oceanic crust (namely, eclogite) as well as sub-KR1 depleted MOR basalt mantle (DMM). Whereas the main source materials for the KR1 tholeiites are presumed to be the DMM-dominant lithology with minor recycled material (Yi et al. 2021). An off-axis seamount chain intersects the ridge at 158.33°E, where the ridge morphology changes from axial rift to axial high. Seventeen sites were identified along the KR1 with the Mujin hydrothermal site, near the centre, having ^{3}HeA of up to 3.8 fmol/kg in water samples (Hahm et al. 2015).

KR2 is a 180 km long segment that progressively deepens from 2,200 m in the west to 2,500 m in the east. An offset divides KR2 into two segments, an eastern rift valley, and a western axial high. The variability of the magma supply is apparently lower than at KR1(Hahm et al. 2015).

(ii) Boomerang Seamount: This active seamount was discovered during a bathymetric survey in 1996. This basaltic seamount lies along the SEIR axis, 18 km NE of Amsterdam Island and marks the site of the Amsterdam - St. Paul hotspot. The seamount rises to within 650 m of the ocean surface and has a 2 km wide summit caldera that is 200 m deep. Rift zones that extend to the SE and N give the seamount its arcuate shape. Water column temperature anomalies above the seamount suggest the presence of hydrothermal activity within the caldera (Johnson et al. 2000).

(iii) Pelagia vent: Pelagia hydrothermal field (26°09.40'S, 71°26.26'E) is located within the neovolcanic zone of the SEIR and near the RTJ at water depth of 3,690 m. Active smoking vents in this site were found to be up to 20 m high on top of a mound of sulfide talus (Noowong et al. 2021). The chimneys have intricate intergrowth of different minerals, while weathered products occur on the outer wall of the vent. The vent fluid flows towards the chimney walls because of abundant pore spaces that have resulted due to aggregates of collomorphic pyrite/marcasite, and sphalerite surrounded by chalcopyrite, lath-shaped pyrrhotite, and amorphous silica, lined with traces of sulfides. All these are evidence of the high-temperature environment prevalent in the area. An inactive chimney depicts replacement of chalcopyrite-isocubanite by secondary copper minerals (Han et al. 2018).

10.3.4 South-West Indian Ridge (SWIR)

The ultraslow-spreading SWIR represents one of the important end-member MOR types because of its very slow and oblique spreading rate of 7-9 mm/yr. The first evidence of high-temperature hydrothermal activity was identified by German et al. (1998). Later a survey was carried out using submersible Shinkai 6500 and temperature anomalies of ~0.1°C were recorded at 31°05'S, 59°00'E and 27°54'S, 64°29'E (Sohrin and Gamo, 1999). The hydrothermal structures are related with E-W trending graben and smaller fissures and cracks (Munch et al. 2000). Geophysical, optical back-scatter and deep-tow side-scan sonar surveys of the rift-valley floor (54° - 67°E) helped to detect six sets of plume signals (German, 2003). A recent morphological and compositional study of the FeMn crusts from a segment of the SWIR indicated distinct hydrothermal signatures from their formation (Kalangutkar et al. 2021). Information about four hydrothermal sites that occur along the SWIR are given below.

(i) Mount Jourdanne: The Melville fracture zone acts as a dividing line for two distinct morphological characteristics. The western side of Melville fracture zone is associated with the highest number of volcanoes per segment indicating a shallower spreading centre (4,400 m) (Mendel et al. 1997). Abyssal tholeiites occur up to the Atlantis II fracture zone while to its east and until the RTJ, the number of volcanoes are less, the spreading centres are deeper (4,800 m) and host sodic and titaniferous glasses (Natland, 1991).

Hydrothermal precipitates in water depths of about 2,960 m close to the top of a neovolcanic ridge (Mount Jourdanne) and weathered reddish-brown SMS of about 5 m are present as small mounds along with small tube-like chimneys. The strongest temperature anomalies of ~0.1°C were recorded at Mt. Jourdanne (27°50.97'S, 63°56.15'E) (Fujimoto et al. 1999). Due to a volcanic heat source and conduits for fluid convection, several extinct hydrothermal sites occur within an area of approximately 0.5 km^2 at a water depth of about 2,941 m within graben or smaller fissures. The chimney edifices rise for approximately 40 to 50 cm from the seafloor and are about 10 cm in diameter. No hydrothermal activity, shimmering waters, chemical anomalies, or biological features were recorded. The summit of Mt. Jourdanne is characterized by E - W trending graben and by basaltic pillows and lava tubes whereas the shallower slopes are dominated by sheet flows (lobate, folded) that are often covered by a thin sediment layer (Munch et al. 2000; Munch et al. 2001).

(ii) Tiancheng and Tianzuo: In Tianzuo hydrothermal field, two inactive, ultramafic-hosted vents (Tiancheng and Tianzuo) occur in the ridge section 63° - 64°E between the Melville fracture zone and RTJ and southwest of the relict Mt. Jourdanne field (Tao et al. 2012). Hydrothermal signatures in sediments reported from 63°E to 68°E (Agarwal et al. 2020)

(iii) Duanqiao and Yuhuang: The Duanqiao and Yuhuang hydrothermal fields are between the Indomed and Gallieni fracture zones at the central volcano along the SWIR (Zhu et al. 2020). Bouguer gravity results indicate the crustal thickness to be between 3 and 10 km (average: 7.5 km) with the maximum crustal thickness of 10 km in the Duanqiao field. This is the thickest crust discovered along the SWIR (Sun et al. 2018). The Duanqiao (inactive) (50.5°E) field lies on an axial highland with a shallow depth of ~1,700 m and relatively flat surrounding terrain (Sun et al. 2018). This field has relict chimneys, massive sulfides, opals, basalts, and metalliferous sediments (Tao et al. 2012). As compared with other areas of the SWIR, abundant siliceous samples such as opals have been recovered that are evident of low-temperature hydrothermal activity (Yang et al. 2019). The Yuhuang (49.2°E) inactive field is located on the south rift wall of segment 29 of the SWIR, approximately 7.5 km from the ridge axis and at water depth ranging from 1,400 to 1,600 m.

(iv) Dragon Horn: The Dragon Horn field with sulfide-bearing vent was identified along an OCC and is located on the south flank of the SWIR segment 28 (~49.7˚E) and it exhibits high-temperature hydrothermal vents that are associated with a major detachment fault system. Twin detachment faults penetrate to a depth of 13 ± 2 km below the seafloor. Dragon Horn is a basalt-hosted active vent field at water depths of 2,700 - 2,900 m comprising of two sulfide-bearing vents: Longqi-1 and Longqi-3 (Tao et al. 2012). The Longqi-1 field is located at segment 28 (~49.7°E) along the Dragon Horn region on the southern flank of the ultra-slow spreading SWIR. Three hydrothermal vents, namely S, M, and N have been confirmed at the Longqi-1 field (Tao et al. 2012). The inactive Longqi-3 field is a hydrothermal plume anomaly site with a possible linear mineralized zone along the detachment fault 2 in serpentinized peridotite along with carbonate sediments. The evidence points to the presence of low-temperature to the east side of the OCC. At the hydrothermal field the calculated Bouguer gravity shows a crustal thickness of ~3 km (Tao et al. 2012).

Considering the above reports it has been shown that areas where SMS occur in the Indian Ocean can be classified into two types: (1) at or near the neovolcanic ridges of the rift valley floor, for example, Meso (Halbach et al. 1998), Mount Jourdanne (Münch et al. 2001), Dodo (Nakamura et al. 2012), Solitaire (Nakamura et al. 2012), Wocan (Wang et al. 2017), Duanqiao (Yang et al. 2017), and Pelagia (Han et al. 2018), and (2) elevated off-axis deposits on the rift valley wall, for example, Edmond (Van Dover et al. 2001), Kairei (Van Dover et al. 2001), Longqi (Tao et al. 2012), 3.69°N (Tao et al. 2013), Yuhuang (Liao et al. 2018), and several sites related with OCCs on the CIR (OCC-3-2, OCC-4-1, and OCC-4-2; Pak et al. 2017).

10.4 THE BLUE ECONOMY OF SEAFLOOR MASSIVE SULFIDES

Although several countries have investigated and even discovered tens of hydrothermal vents in the ocean, surprisingly, only a handful of countries are registered contractors with the ISA (erstwhile UNCLOS). In contrast to the 19 contractors for polymetallic nodules in the Pacific and Indian oceans, there are only seven contractors for exploration of the SMS. This is even though the SMS deposits occur at relatively shallower water depths than the nodules (>5,000 m). The contractors for SMS in the Indian Ocean are one each in the SWIR and CIR, and five in the MAR. These contractors are India, China, Germany, and Korea. The three contractors along the MAR are Poland, France and Russia.

The National Centre for Polar and Ocean Research (NCPOR, Goa India) (erstwhile the National Centre for Antarctica and Ocean Research) under the support of the Ministry of Earth Sciences initiated a mission-mode multi-disciplinary program on exploration of the SMS along the SWIR and CIR. In 2014, India obtained a 15-year licence from the ISA to explore 10,000 km of the CIR and SWIR for SMS and in 2016 India signed a 15-year exploration contract which would expire on 25th March 2031. The first cruise was undertaken on 12th Jan 2017 along segments of the CIR and SWIR. Multi-disciplinary efforts were made to locate potential SMS deposits. Seamounts are easier to sample since these may occur at shallow water depth (500 m) and host ferromanganese (FeMn) oxides with significant contents of cobalt (~1%). Such seamounts have been targeted for mining by five contractors: Korea, Japan and Russia in the Pacific Ocean, Brazil in the South Atlantic Ocean and China in the Western Pacific Ocean (Mukhopadhyay et al. 2018). In the Indian Ocean, the Afanisy-Nikitin Seamount (ANS) has significant cobalt (Co 0.3-0.9%, average: 0.65%), rare earth elements and platinum (200 - 900 ppb) (Rajani et al. 2005; Balaram et al. 2012). But beyond this preliminary work, the ANS has so far not been earmarked for exploitation by India.

Sustainable and profitable mining, either on land or from the deep-seas, involve one or more of the 5Es: Exploration, Environmental studies, Exploitation, Enrichment and Economics. A successful completion of all these 5Es could result in 'Minerals to Market.' We discuss the importance of the BE for India (as a contractor) in her endeavour to comprehend the potential economic viability and related issues of the SMS deposits.

10.4.1 Exploration

In the late eighties and early nineties, ridge research in India was mostly individual driven (for example, Mukhopadhyay and Iyer, 1993) and there was an absence of integration. Hence, to have a synergy at a national level, in 1997 the Council of Scientific and Industrial Research-National Institute of Oceanography (CSIR-NIO), Goa initiated a major programme, 'Tectonic and Oceanic Processes Along the Indian Ridge System and Backarc Basins.' Simultaneously, the InRidge (India's Ridge Research initiative) was formed and India became an Associate Member in the global

InterRidge body. InRidge provided opportunities to individuals and institutions to collaborate, save funds and resources, help avoid duplication of research efforts, share samples, ship time and train researchers and students. The other reasons were lack of data pertaining to the IORS and their easy accessibility from Indian shores.

The areas of studies chosen under the InRidge were the CR, CIR and ABAB, to understand tectonic architecture, transform faults (TF), ridge-transform interaction (RTI), incipient triple junction formation, interaction of the wide deformation zone, seamounts, petrological variations, and most importantly, to search for hydrothermal vents. The Geological Survey of India (GSI) also conducts its studies in the CR and ABAB. Although India started her ridge studies much later than other countries who have extensively studied the MAR, SWIR, EPR and other areas in the world's oceans, nevertheless much impact and many findings have resulted from the InRidge. Currently, investigations are underway along segments of the CR, CIR and SWIR and plans are afoot to examine the SEIR.

The hydrothermal fields along the SWIR, SEIR, CIR and CR are generally sited within axial rift valleys or rift flanks on segment centers, hence these need to be targeted to locate hydrothermal vents. In the exploratory work, India could consider collaborating with the IORA countries such as Sri Lanka, Maldives, Mauritius, Seychelles, and Madagascar who would assist to expedite the expeditions to the IORS in a faster, easier and less expensive manner. This effort could lead to training of personnel, job opportunities and development in scientific and port infrastructure and economic growth in the collaborating countries.

10.4.2 Environment

Extracting the SMS deposits could be a challenging task. This is because mining will inevitably affect the environment, but several metals from the SMS are required in technologies that are vital to society to have a low-carbon future and to achieve the global sustainable development goals (Lusty and Murton, 2018). It is mandated that under Regulation 32 the Contractors need to undertake environmental baseline studies (ISA, 2013) as recommended and outlined by ISA's Legal and Technical Commission (LTC). The LTC stipulates that 'the best available technology and methodology for sampling should be used in establishing baseline data for environmental impact assessments.' Besides following the protocols, plausible solutions and mitigatory measures also have to be outlined by the contractor.

Before, during and after mining, an array of complex environmental impacts need to be assessed. These would include physical oceanography, sediment characteristics (physical and chemical), the sinking rate of particles, the aggregation of particles, toxic discharges, biological studies (microbes to mammals), biodiversity, ecosystem functioning, hydrodynamic plume modelling, noise and light hazards, amongst others (Billett et al. 2019). Noowong et al. (2021) reported the molecular composition of dissolved organic matter (DOM) of Kairei (CIR) and Pelagia (SEIR) vents. The vent fluids (>330°C) were extremely rich in dissolved Fe, Si, K, Li, Mn and Zn compared to the seawater. The DOM from these fluids was different than that from diffuse fluids and plumes, which had a predominant signature of the seawater DOM.

Hydrothermal vents shelter a variety of biota that rely on microbial chemosynthesis by using hydrogen sulfide and methane in the hot vent fluid as sources of energy (Van Dover, 2000). Globally, about 600 of such sites have been located (Beaulieu and Szafrański, 2020) and most of these are in the Pacific and Atlantic Oceans (Thaler and Amon, 2019). The active vent ecosystem is a rare habitat and comprises an estimated 50 km^2, that is < 0.00001% of the Earth's surface area (Van Dover et al. 2018). Therefore, mining could potentially harm the biota that are endemic around the vents.

The deep-sea environment could also change in other ways during mining operations. For example, a deep drilling operation at the Iheya North hydrothermal field (Okinawa Trough, Pacific Ocean) revealed that the vent-clam/soft sediment habitat transforms into a crust with higher temperature flow and the presence of bacterial mat and squat lobsters (Nakajima et al. 2015). On the other hand, when drilling took place at ODP Leg 158 in the TAG area of the MAR there was hardly any change in the nature of the shrimp-dominated vents (Copley et al. 1999, 2016). Under such circumstances it is difficult to foresee the damage, or lack of it, at hydrothermal vents.

Both terrestrial and deep-sea mining influence the environment in different ways and more so when sea-minerals are mined. This is because during mining the water column, bottom water, biota (bottom-dwelling, surface and water column inhabitants) and bottom sediments would be altered. Therefore, after exploration and prior to exploitation, an in-depth study is required concerning the Environment Impact Assessment (EIA) and Environment Monitoring and Planning (EMP). The EIA and EMP are multidisciplinary approaches to address the concerns that the stakeholders and people would have once mining starts. Baseline data need to be obtained, namely, observations and measurements of several parameters of geological, biological, physical, and chemical nature, of the water, biota, and sediments. The data, samples, and observations must be validated, compared, and checked for variations in reference (control) and test (experimental) areas. The investigations could range from a few days to 2 - 3 years and be a continuing process, even after mining.

Filho et al. (2021) reviewed the potentials and risks of deep seabed mining by considering the legal aspects and environmental impact. During mining, the seabed could be significantly disturbed, the creation of sediment plumes, and these together with light and noise pollution would affect the surface, benthic, meso, and bathypelagic zones. A systems approach to adaptive management was proposed by Hyman et al. (2021) that could help to guide and better manage the environmental aspects deep-sea mineral extraction.

Except for routine geological, biological and seawater sampling at the licensed site of the SWIR, India has not reached the stage where EIA/EMP tasks are being carried out. But the data so far collected would help to undertake the detailed EIA work in the future.

10.4.3 Exploitation

During the mid-1970s successful pre-pilot mining and metallurgical testing operations were carried out at the Atlantis II deep site. It was then presumed that very soon there would be a clamour to mine for deep-sea minerals from the world's ocean. To-date, this dream of the scientific community is unrealised due to factors other than technological advancements in mining. Further we need to allay the growing global fear for the marine environment, both by people and regulatory bodies such as the ISA. Despite such concerns, there is now a renewed interest ini the exploitation of the SMS deposits given the ever-growing global population, industrialisation, an enhanced demand for metals, and geopolitical issues, amongst others.

Deep-sea mining is an expensive proposition as it is essential not only to have high resolution mapping techniques but also to fabricate equipment that can withstand the erosive effect of the seawater and hydrostatic pressures. In addition, low-cost autonomous or remotely operated vehicles (AUV/ROV) would be necessary to locate and evaluate SMS deposits. The mined materials that are recovered by the mother ship must be transported to onshore processing laboratories using supply vessels. Presently some limited mining systems exist but not for commercial operations as is the case for nearshore placer deposits that are mined by a few countries, including India. Once the mining lease and environmental clearances are obtained then the SMS deposits of the Solwara 1 site in the Bismarck Sea (Papua New Guinea) could be the first to be commercially mined. The SMS deposits are 50 km from land and at a water depth of 1,600 km. The inferred total mineral resource is ~1.54 million tonnes with a grade of 6% of gold grams/tonne and 8% copper (Lipton, 2008).

The other constraints to seabed mining are the availability of ore and mineral deposits on land that are similar to the marine deposits, procurement of a license and its yearly renewal at a huge price from the ISA to explore and exploit marine resources, and a large capital investment which is usually only possible either by consortia or by governments or through partnerships. India has developed a nodule mining system, a soil tester and an ROV (ROSUB 6000), all of which are operable at 6,000 m water depth. Work is underway to develop a battery-operated manned submersible that would have an endurance of 12 hours and dive at least 6,000 m (www.niot.org). Recently the Indian government has approved the 'Deep Ocean Mission,' in which there are plans to develop suitable mining systems for the SMS and polymetallic manganese nodules.

India could collaborate with some of the IORA or advanced countries that may have expertise to jointly develop and produce deep-sea mining and other ancillary systems. The efforts would mutually benefit the countries in terms of exchange of scientific and technological ideas, the creation of employment opportunities, a shared and reduced cost of manufacturing of machinery, and the hastening of the process of mining the SMS deposits, amongst others.

10.4.4 Enrichment

The hydrothermal deposits are a concoction of various metals, oxides, sulfides and sulfates of iron, copper, nickel, cobalt, zinc, lead, gold, silver, barium, silica amongst others. The extraction of a particular metal from such a conglomeration is difficult unlike the processes that help to separate 3 (copper, cobalt nickel) or 4 metals (copper, cobalt, nickel, and manganese) from polymetallic nodules. Several metallurgical techniques must be developed or existing ones need to be refined to separate as many of the metals as possible from the SMS. This could involve the setting-up of large metallurgical plants that would require extensive treatment and efficient disposal of their chemical effluents so as not to contaminate the subsurface and groundwaters. The gangue that would be produced during metal extraction needs to be either examinedto see if it could be put to some use or disposed of. Noise and air pollution produced from the beneficiation plants must be alleviated as much as possible.

Once the flow charts to recover the metals from the SMS are finalized then as a part of the BE initiative, India could establish ore beneficiation plants in one or more of the IORA countries that are near the area. This step would help to save the cost of transporting the SMS from the SWIR which is located tens of kilometres from India, reduction in the carbon footprint, and help to boost metal production. The host country could benefit by way of improved or new infrastructure, creation of jobs, advances in science and technology, and financial gain through foreign investments.

10.4.5 Economics

The overall accumulation of the SMS in the MOR is estimated to be ~6×10^8 tonnes and of this, 86% is accounted for by deposits present along slow- and ultraslow-spreading ridges (Hannington et al. 2011). It has been reported that a majority of hydrothermal fields with more than 1 million tonnes are found along such ridges that have spreading rates between 20 and 55 mm/yr and <20 mm/yr, respectively (Dick et al. 2003). So far, a little more than 20 fields have been found and confirmed on ultraslow-spreading ridges *(www.vents-data.interridge.org/)* and among these, only for the Mount Jourdanne deposit (SWIR), was the size reported. The estimated SMS is <3,000 tonnes, using the area versus tonnage relationship for the Solwara-1 deposit as a reference, and this is much smaller than expected (Hannington et al. 2011). Therefore, we need more data to demarcate the distribution and content of SMS on ultraslow-ridges.

The Yuhuang-1 hydrothermal field (YHF), situated on the SWIR, has two SMS deposits that are ~500 m apart, one in the SW and other in NE. Calculations reveal that the total volume of SMS in the YHF is ~10.6×10^6 tonnes, with at least ~7.5×10^5 tonnes of Cu and Zn and ~18 tonnes of Au. Accounting for the coverage of layered hydrothermal sediment together with sulfide-rich breccias and underlying massive sulfide deposits, the maximum total mass was estimated at ~45.1×10^6 tonnes. Apparently, the YHF is one of the largest SMS deposits worldwide and reaffirms that ultraslow-spreading ridges have the greatest potential to form large-scale SMS deposits (Yu et al. 2021).

It is tempting for a country or consortia to follow the above 4Es in the hope of extracting several metals simultaneously from SMS deposits and make a handsome profit in the long term. Reportedly, the metals in the SMS deposits may sometimes exceed terrestrial reserves that are now economically mined (Hein et al. 2013). After having been granted the license and strictly adhering to the ISA guidelines to mine the SMS deposits, a critical analysis of the cost-benefit and the multiple issues involved with it need to be worked out by the investors. The investors must account for factors such as capital costs (mother ship, supply vessels), manpower, salaries, daily expenses, hiring/purchase/replacement of mining equipment, transport of personnel and mined ores to land, establishing an onshore facility for metal extraction by following all protocols of EIA and EMP, fluctuating market values of the metals, import-export of the metals, and various other known/unknown factors. Importantly, the profits could fluctuate depending on distribution and resource estimates of the SMS deposits and whether active or inactive vents would be mined.

The investors must consider the fact that future discovery of new ore deposits on land could substantially reduce their profits. In the above constraints we have not accounted for the vagaries of nature that could hamper mining operations. Although it is predicted that by 2030 about 10% of global minerals could be recovered from the ocean floor (European Commission, 2012), we still have a long way to go to make deep-sea mining a profitable venture.

Considering a host of parametres (abundance, grade, topography, metal prices, infrastructure, capital costs, and the like), it was estimated that by mining the Central Indian Ocean Basin (CIOB) polymetallic nodules (water depth 5,000 m) that profits could be made from the 8th year of a 25 year life of the mine (Mukhopadhyay et al. 2019). In the case of shallow-seated SMS deposits perhaps the profits could be realized much earlier provided that the other 4Es have been properly addressed.

10.5 CONCLUSION

Currently, the world is managing with its available land resources but a time could come when it needs to turn to the oceans for mining useful metals and minerals. But the day is not far off when countries will be able to recover marine minerals when technologies are developed, environmental concerns are addressed and mechanisms for sustainable marine mining are set in place. These factors could be accelerated, and the cost reduced, if countries and global corporates worked in unison instead of working in isolation. Regarding seabed mineral exploration, India is quite ahead in the game with respect to its neighbouring countries and, indeed most IORA countries. This is because the Indian Ocean is easily accessible, its availability of large quantities of human resources (scientific, skilled, unskilled), technological advancements for exploration, environmental studies, exploitation, and its ore beneficiation plants, amongst other favourable factors.

After the Goa Declaration (2015), the Indian government seriously took up several initiatives to identify and boost blue economy sectors, with emphasis on marine minerals. The National Institute of Transforming India (NITI) is working hand-in hand with different stakeholders and the Ministry of Earth Sciences to successfully implement a sustainable use of several blue minerals (placers, SMS, polymetallic nodules). This is in tune with the Government's policy statement which is, 'The blue economy refers to the exploring and optimizing of the potential of the oceans and seas which are under India's legal jurisdiction for socio-economic development while preserving the health of the oceans.'

Several recommendations were made by Nayak (2019) to the government of India. Some of these are to expedite technology development for exploration, and the like, the setting up of a national placer mission, financial and human resources, exploration rights for cobalt, a comprehensive study of the Andaman and Nicobar Islands, protecting marine biodiversity, and to establish an appropriate institutional framework to implement the BE activities. It was estimated that the size of the BE in India, measured in Gross Value Added (GVA), in 2016–17 was US$81.8 billion. Currently, the magnitude of the BE is akin to several coastal nations although in some countries (like Malaysia and

Mauritius), the input of BE to Gross Domestic Product (GDP) is quite significant. In India the GVA steadily rose from 3% 2012 - 13 to 10.5% in 2015 - 16. The present contribution of BE to the GDP is ~4% but this could surge if we consider outputs from all the marine sectors or marine-related activities (Rajeevan, 2019).

We suggest that India could establish an independent Ministry of Blue Economics that would chalk out programmes, outline work plans, take policy decisions and successfully implement the BE by networking with the other sectors of the BE. By doing so, the blue minerals could be sustainably resourced in an environmentally-friendly manner and thus substantially contribute to India's projected economy of US$10 trillion by 2030, despite the recent set-backs caused by the ongoing COVID-19.

ACKNOWLEDGEMENTS

We acknowledge Prof. Dr. Md. Nazrul Islam for the invitation to contribute this chapter. We thank Ms. Mansi Shinde during the preparation of Table 10.1. We also acknowledge the support of Goa University and DM college during the preparation of the chapter.

REFERENCES

Agarwal, D. K. Roy, P. Prakash, L. S. and Kurian, P.J. 2020. Hydrothermal signatures in sediments from eastern Southwest Indian Ridge 63 E to 68 E. *Marine Chemistry*, 218: 103732.

Balaram, V. Banakar, V. K. Subramanyam, K. S. V. Roy, P. Satyanarayan, M. Ram Mohan, M. and Sawant, S. S. 2012. Yttrium and rare earth element contents in seamount cobalt crusts in the Indian Ocean. *Current Science*, 103: 1334–1338.

Banerjee, R. and Iyer, S. D. 1991. Petrography and chemistry of basalts from the Carlsberg Ridge. *Journal of Geological Society of India*, 38: 369–386.

Banerjee, R. and Iyer, S. D. 1993. A note on sulfide-oxide mineralisation in Carlsberg Ridge basalts. *Journal of Geological Society of India*, 42: 579–584.

Banerjee, R. and Iyer, S. D. 2003. Genetic aspects of basalts from the Carlsberg Ridge. *Current Science* (Special Section on Mid-Oceanic Ridges), 85: 299–305.

Banerjee, R. and Ray, D. 2013. Metallogenesis along the Indian Ocean Ridge System. *Current Science* (Special Section on Mid-Oceanic Ridges), 85: 321–327.

Barnes, H. L. and Rose, A. W. 1998. Origins of hydrothermal ores. *Science*. 279: 2064–2065.

Baturin, G. N. and Rozanova, T. V. 1975. Ore mineralization in the rift zone of the Indian Ocean. In: Vinogradov, A.P. and Udintsev, G.B. (eds), *Rift Zones of the World Oceans*. Wiley, New York and Israel Prog Sci Trans, pp. 431–441.

Beaulieu, S. E. and Szafrański, K. M. 2020. InterRidge global database of active submarine hydrothermal vent fields version 3.4. *PANGAEA*. doi:10.1594/PANGAEA.917894 Chapman, A.S.A. Beaulieu, S.E. Colaço, A. Gebruk, A.V. Hilario A. Kihara.

Bierlein, F. P. Groves, D. I. and Cawood, P. 2009. Metallogeny of accretionary orogens—the connection between lithospheric processes and metal endowment. *Ore Geology Reviews*, 36(4): 282–292.

Billett, D. S. M, Jones, D. O. B. and Weaver, P. P. E. 2019. Improving environmental management practices in deep-sea mining. *Environmental Issues of Deep-Sea Mining*, 403–446.

Chen, D. Tao, C. Wang, Y. Chen, S. Liang, J. Liao, S. and Ding, T. 2021. Seafloor Hydrothermal activity around a large non-transform discontinuity along ultraslow-spreading Southwest Indian Ridge (48.1–48.7°E). *Journal of Marine Science and Engineering*, 9(8): 825.

Chen, J. Tao, C. Liang, J. Liao, S. Dong, C. Li, H. Li, W. Wang, Y. Yue, X. and He, Y. 2018. Newly discovered hydrothermal fields along the ultraslow-spreading Southwest Indian Ridge around 63°E. *Acta Oceanologica Sinica*, 37(11): 61–67.

Chen, X. Sun, X. Wu, Z. Wang, Y. Lin, X. and Chen, H. 2021. Mineralogy and geochemistry of deep-sea sediments from the ultraslow-spreading Southwest Indian ridge: implications for hydrothermal input and igneous host rock. *Minerals*, 11(2): 138.

Chen, Y. Han, X. Wang, Y. and Lu, J. 2020. Precipitation of calcite veins in serpentinized harzburgite at Tianxiu hydrothermal field on Carlsberg Ridge (3.67° N), Northwest Indian Ocean: implications for fluid circulation. *Journal of Earth Science*, 31(1): 91–101.

Choi, H. Kim, S. S. and Park, S. H. 2013. Interpretation of bathymetric and magnetic data from the eastern-most segment of Australian-Antarctic Ridge, 156°–161°E. *American Geophysical Union Fall Meeting Abstracts*, 2013: T13A–T2498.

Copley, J. Tyler, P. VanDover, C. Schultz, A. Dickson, P. Singh, S. and Sulanowska, M. 1999. Effects of ODP drilling on the TAG hydrothermal vent community, 26 N Mid-Atlantic Ridge. *Marine Ecology*, 20: 291–306.

Copley, J. T. Marsh, L. Glover, A. G. Hühnerbach, V. Nye, V. E. Reid, W .D. K. Sweeting, C. J. Wigham, B. D. Wiklund, H. 2016. Ecology and biogeography of megafauna and macrofauna at the first known deep-sea hydrothermal vents on the ultraslow-spreading Southwest Indian Ridge. *Scientific Reports*, 6(1): 39158. doi: 10.1038/srep39158.

Degens, E. T. and Ross, D. A. 1969. *Hot Brines and Recent Heavy Metal Deposits in the Red Sea: Geochemical and Geophysical Account*. Springer-Verlag, Berlin, Heidelberg, p. 600. doi: 10.1007/978–3-662–28603–6.

DeMets, C. Gordon, R. G. Argus, D. F. and Stein, S. 1990. Current plate motions. *Geophys. J. Int*. 101: 425– 478.

Dhawaskar, P. Ganguly, S. Mukhopadhyay, R. Manikyamba, C. Iyer, S. D. Karisiddaiah, S. M. and Mahender, K. 2020. Geochemical heterogeneity along the Vema Fracture Zone, Indian Ocean: mixing of melts from the reunion plume and the Central Indian Ridge. *Geological Journal*, 55: 330–343. https://doi.org/10.1002/gj.3395.

Dick, H. J. B. Lin, J. and Schouten, H. 2003. An ultraslow-spreading class of ocean ridge. *Nature*, 426(6965): 405–412.

Drolia, R. K. Iyer, S. D. Chakraborty, B. Kodagali, V. N. Ray, D. Misra, S. Andrade, R. Sarma, K. V. L. N. S. Rajasekhar, R. P. and Mukhopadhyay, R. 2003. The Northern Central Indian Ridge: geology and tectonics of fracture-zones dominated spreading ridge segments. *Current Science* (Special Section on Mid-Oceanic Ridges), 85: 290–298.

European Commission. 2012. *Blue Growth: Opportunity for Marine and Maritime Sustainable Growth*. Communication from the Commission to the European Parliament, the Council. The European Economic and Social Committee of the Regions. European Union, Luxembourg, 494 final, pp. 12. doi: 10.2771/43949.

Filho, W. L. Abubakar, I. R. Nunes, C. Platje, J. Ozuyar, P. G. Will, M. Nagy, G. J. Al-Amin, A. Q. Hunt, J. D. and Li, C. 2021. Deep seabed mining: a note on some potentials and risks to the sustainable mineral extraction from the oceans. *Journal of Marine Science and Engineering*, 9: 521. https://doi.org/10.3390/jmse9050521.

Franklin, J. M. Gibson, H. L. Jonasson, I. R. and Galley, A. G. 2005. Volcanogenic massive sulfide deposits. In Hedenquist, J. W. Thompson, J. F. H. Goldfarb, R. J. and Richards, J. P. (eds), *Economic Geology One Hundredth Anniversary Volume: Society of Economic Geologists*, pp. 523–560.

Fouquet, Y. 1997. Where are the large hydrothermal sulfide deposits in the oceans? *Proceedings of the Royal Society A*, 355(1723): 427–441.

Fujii, M. and Okino, K. 2018. Near-seafloor magnetic mapping of off-axis lava flows near the Kairei and Yokoniwa hydrothermal vent fields in the Central Indian Ridge. *Earth, Planets and Space*, 70(1): 1–17.

Fujii, M. Okino, K. Sato, T. Sato, H. and Nakamura, K. 2016. Origin of magnetic highs at ultramafic hosted hydrothermal systems: insights from the Yokoniwa site of Central Indian Ridge. *Earth and Planetary Science Letters*, 441: 26–37.

Fujimoto, H. Cannat, M. Fujioka, K. Gamo, T. German, C. Mével, C. Münch, U. Ohta, S. Oyaizu, M. Parson, L. Searle, R. Sohrin, Y. and Yama-ashi, T. 1999. First submersible investigations of mid-ocean ridges in the Indian Ocean. *InterRidge*, 8: 22–24.

Gallant, R. M. and Von Damm, K. L. 2006. Geochemical controls on hydrothermal fluids from the Kairei and Edmond Vent Fields, 23°–25°S, Central Indian Ridge. *Geochemistry, Geophysics, Geosystems*, 7: 6, Q06018, doi: 10.1029/2005GC001067.

Gamo, T. Chiba, H. Yamanaka, T. Okudaira, T. Hashimoto, J. Tsuchida, S. Ishibashi, J. Kataoka, S. Tsunogai, U. Okamura, K. Sano, Y. and Shinjo, R. 2001. *Earth and Planetary Science Letters,* 193: 371–379.

Gamo, T. Nakayama, E. Shitashima, K. Isshiki, K. Obata, H. Okamura, K. Kanayama, S. Oomori, T. Koizumi, T. Matsumoto, S. and Hasumoto H. 1996. Hydrothermal plumes at the Rodriguez triple junction, Indian ridge. *Earth and Planetary Science Letters*, 142: 261–270.

Garuti, G. Bartoli, O. Scacchetti, M. and Zaccarini, F. 2008. Geological setting and structural styles of Volcanic Massive Sulfide deposits in the Northern Apennines (Italy): evidence for seafloor and sub-seafloor hydrothermal activity in unconventional ophiolites of the Mesozoic Tethys. *Boletin de la Sociedad Geologica Mexicana*, 60/1: 121–145.

German, C. R. 2003. Hydrothermal activity on the eastern SWIR (50°–70°E): Evidence from core-top geochemistry, 1887 and 1998. *Geochemistry, Geophysics, Geosystems*, 4: 7, 9102. doi: 10.1029/2003GC000522.

German, C. R. Baker, E. T. Mevel C. Tamaki, K. and the FUJI Science Team. 1998. Hydrothermal activity along the southwest Indian ridge. *Nature*, 395: 490–493.

Hahm, D. Baker, E. T. Rhee, T.S. Won, Y. J. Resing, J. A. Lupton, J. E. Lee, W. K. Kim, M. Park, S. Y. 2015. First hydrothermal discoveries on the Australian-Antarctic Ridge: Discharge sites, plume chemistry, and vent organisms. *Geochemistry, Geophysics, Geosystems*, 16: 3061–3075.

Halbach, M. Halbach, P. and Luders, V. 2002. Sulfide impregnated and pure silica precipitates of hydrothermal origin from the Central Indian Ocean. *Chemical Geology*, 182: 357–375.

Halbach, P. Blum N. Munch U. Pluger W. Garbe-Schonberg D. and Zimmer, M. 1998. Formation and decay of a modern massive sulfide deposit in the Indian Ocean. *Mineralium Deposita*, 33: 302–309.

Han, Y. Gonnella, G. Adam, N. Schippers, A. Burkhardt, L. Kurtz, S. Schwarz-Schampera, U. Franke, H. and Perner, M. 2018. Hydrothermal chimneys host habitat-specific microbial communities: analogues for studying the possible impact of mining seafloor massive sulfide deposits. *Scientific Reports*, 8(1): 1–12.

Hannington, M. Jamieson, J. Monecke, T. Petersen, S. and Beaulieu, S. 2011. The abundance of seafloor massive sulfide deposits. *Geology*, 39(12): 1155–1158.

Hein, J. R. Mizell, K. Koschinsky, A. and Conrad, T. A. 2013. Deep-ocean mineral deposits as a source of critical metals for high-and green-technology applications: comparison with land-based resources. *Ore Geology Reviews*, 51: 1–14.

Herzig, P. M. and Plüger, W. L. 1988. Exploration for hydrothermal activity near Rodriguez Triple Junction, Indian Ocean. *Canadian Mineralogist*, 26: 721–736.

Hyman, J. Stewart, R. A. and Sahin, O. 2021. Adaptive management of deep-seabed mining projects: a systems approach. *Integrated Environmental Assessment and Management*, doi: https://doi.org/10.1002/ieam.4395.

ISA. 2013. Recommendations for the guidance of contractors for the assessment of the possible environmental impacts arising from exploration for marine minerals in the Area. ISBA/LTC/19/8. https://isa.org.jm/sites/default/ files/ files/documents/isba-19ltc8_0.pd.

Iyer, S. D. and Banerjee, R. 1993. Mineral chemistry of Carlsberg Ridge basalts at 3° 35'–3° 41' N. *Geo-Marine Letters*, 13: 153–158.

Iyer, S. D. and Ray, D. 2003. Structure, tectonic and petrology of mid-oceanic ridges and the Indian scenario. *Current Science* (Special Section on Mid-Oceanic Ridges), 85: 277–289.

Ji, F. Zhou, H. Yang, Q. Gao, H. Wang, H. and Lilley, M. D. 2017. Geochemistry of hydrothermal vent fluids and its implications for subsurface processes at the active Longqi hydrothermal field, Southwest Indian Ridge. *Deep Sea Research Part I: Oceanographic Research Papers*, 122: 41–47.

Johnson, K. T. M. Graham, D. W. Rubin, K. H. Nicolaysen, K. Scheirer, D. S. Forsyth, D. W. Baker, E. T. and Douglas-Priebe, L. M. 2000. Boomerang Seamount: the active expression of the Amsterdam–St. Paul hotspot, Southeast Indian Ridge. *Earth and Planetary Science Letters*, 183: 245–259.

Kalangutkar, N. G. Kurian, P. J. and Iyer, S. D. 2021. Characterization of ferromanganese crusts from the Central and South West Indian ridges: evidence for hydrothermal activity, *Marine Georesources and Geotechnology*, doi: 10.1080/1064119X.2021.1886205.

Kawagucci, S. Miyazaki, J. Noguchi, T. Okamura, K. Shibuya, T. Watsuji, T. Nishizawa, H. Watanabe, K. Okino, N. Takahata, Y. Sano, K. Nakamura, A. Shuto, M. Abe, Y. Takaki, T. Nunoura, M. Koonjul, M. Singh, G. Beedessee, M. Khishma, V. Bhoyroo, D. Bissessur, L.S. Kumar, D. Marie, K. Tamaki, K. and Takai, K. 2016. Fluid chemistry in the Solitaire and Dodo hydrothermal fields of the Central Indian Ridge. *Geofluids*, 16(5): 988–1005.

Kempe, D. R .C. and Easton, A. J. 1974. Metasomatic garnets in calcite (micarb) chalk at SITE 251, Southwest Indian Ocean. *Deep Sea Drilling Project, Initial Reports DSDP*, 26: 593–599. doi: 10.2973/dsdp.proc.26.1974.

Kim, J. Son, S. K. Kim, D. Pak, S. J. Yu, O. H. Walker, S.L. Oh, J. Choi, S. K. Ra, K. Ko, Y. Kim, K. H. Lee, J. H. and Son, J. 2020. Discovery of active hydrothermal vent fields along the Central Indian Ridge, 8–12 S. *Geochemistry, Geophysics, Geosystems*, 21(8): e2020GC009058.

Kumagai, H. Nakamura, K. Toki, T. Morishita, T. and Okino, K. 2008. Geological background of the Kairei and Edmond hydrothermal fields along the Central Indian Ridge: implications of their vent fluids' distinct chemistry. *Geofluids*, 8: 239–251.

Kutina, J. 1983. Global tectonics and metallogeny: deep roots of some ore-controlling fracture zones. A possible relation to small-scale convective cells at the base of the lithosphere? *Advances in Space Research*, 3(2): 201–214.

Liao, S. Tao, C. Li, H. Barriga, F. J. A. S. Liang, J. Yang, W. Yu, J. and Zhu, C. 2018. Bulk geochemistry, sulfur isotope characteristics of the Yuhuang-1 hydrothermal field on the ultraslow-spreading Southwest Indian Ridge. *Ore Geology Reviews*, 96: 13–27.

Liao, S. Tao, C. Zhu, C. Li, H. Li, X. Liang, J. Yang, W. and Wang, Y. 2019. Two episodes of sulfide mineralization at the Yuhuang-1 hydrothermal field on the Southwest Indian Ridge: insight from Zn isotopes. *Chemical Geology*, 507: 54–63.

Lipton, I. 2008. Mineral resource estimate, Solwara 1 project, Bismarck Sea, Papua New Guinea: NI43–101 Technical Report for Nautilus Minerals Inc. http://nautilusminerals.com/i/pdf/2008–02–01_Solwara1_43–101.pdf (July 2011).

Lusty, P. A. J. and Murton, B. J. 2018. Deep-ocean mineral deposits: metal resources and windows into earth processes. *Elements*, 301–306, doi: 10.2138/gelements.14.5.301.

Mendel, V. and Sauter, D. 1997. Seamount volcanism at the super slow-spreading Southwest Indian Ridge between 57° and 70°. *Geology*, 25(2): 99–102.

Mudholkar, A.V. Kodagali, V. N. Kamesh Raju, K. A. Valsangkar, A. B. Ranade, G. H. and Ambre, N. V. 2002. Geomorphological and petrological observations along a segment of slow-spreading Carlsberg Ridge. *Current Science*, 82: 982–989.

Murton, B. J. Baker, E. T. Sands, C. M. and German, C. R. 2006. Detection of an unusually large hydrothermal event plume above the slow-spreading Carlsberg Ridge: NW Indian Ocean. *Geophysical research letters*, *33*(10) L10608, doi:10.1029/2006GL026048.

Mukhopadhyay, R. and Iyer, S. D. 1993. Petrology of tectonically segmented Central Indian Ridge. *Current Science*, 65: 623–628.

Mukhopadhyay, R. Ghosh, A. K. and Iyer, S. D. 2018. *The Indian Ocean Nodule Field: Geology and Resource Potential*. 2nd edition, Elsevier, Amsterdam, pp. 413.

Mukhopadhyay, R. Iyer, S. D. Ray, D. Karisiddaiah, S. M. and Drolia, R. K. 2015. Morphotectonic and petrological variations along the southern Central Indian Ridge. *International Journal Earth Sciences* (Geol Rundsch), 105: 905–920. doi: 10.1007/ s00531–015–1193-z.

Mukhopadhyay, R. Loveson, V. J. Iyer, S. D. and Sudarsan, P. K. 2020. *Blue Economy of the Indian Ocean: Resource Economics, Strategic Vision, and Ethical Governance*. CRC Press, Boca Raton, Florida, USA, pp. 297.

Mukhopadhyay, R. Naik, S. De Souza, S. Dias, O. Iyer, S. D. and Ghosh, A. K. 2019. The economics of mining seabed manganese nodules: a case study of the Indian Ocean nodule field. *Marine Georesources and Geotechnology*, doi: 10.1080/1064119X.2018. 1504149.

Munch, U. Blum, N. and Halbach, P. 1999. Mineralogical and geochemical features of sulfide chimneys from the MESO zone, Central Indian Ridge. *Chemical Geology*, 155: 29–44.

Münch U. Halbach P. and Fujimoto H. 2000. Sea-floor hydrothermal mineralization from the Mt. Jourdanne*,* Southwest Indian Ridge*. JAMSTEC. Journal of Deep Sea Research*, 16: 125–132.

Munch, U. Lalou, C. Halbach, P. and Fujimoto, H. 2001. Relict hydrothermal events along the super-slow Southwest Indian spreading ridge near 63°56’E—Mineralogy, chemistry and chronology of sulfide samples. *Chemical Geology*, 177: 341–349.

Nakajima, R. Yamamoto, H. Kawagucci, S. Takaya, Y. Nozaki, T. Chen, C. Fujikura, K. Miwa, T. and Takai, K. 2015. Post-drilling changes in seabed landscape and megabenthos in a deep-sea hydrothermal system, the Iheya North field, Okinawa trough. *PLoS One*, 10: e0123095. http://dx.doi.org/10.1371/journal.pone.0123095.

Nakamura, K. Watanabe, H. Miyazaki, J. Takai, K. Kawagucci, S. Noguchi, T. Nemoto, S. Watsuji, T. Matsuzaki, T. Shibuya, T. Okamura, K. Mochizuki, M. Orihashi, Y. Ura, T. Asada, A. Marie, D. Koonjul, M. Singh, M. Beedessee, G. Bhikajee, M. and Tamaki, K. 2012. Discovery of new hydrothermal activity and chemosynthetic fauna on the Central Indian Ridge at 18–20 S. *PLoS One*, 7(3): e32965.

Natland, J. 1991. Indian Ocean crust. In: Floyd, P.A. (eds), *Oceanic Basalts*. Springer, Boston, MA. https://doi.org/10.1007/978–1-4615–3540–9_12.

Nayak, S. 2019. *Report of Blue Economy Working Group on Coastal and Deep-Sea Mining and Offshore Energy*. Ministry of Earth Sciences, New Delhi, India, p. 80 .

Noowong, A. Gomez-Saez, G. V. Hansen, C. T. Schwarz-Schampera, U. Koschinsky, A. and Dittmar, T. 2021. Imprint of Kairei and Pelagia deep-seahydrothermal systems (Indian Ocean) on marine dissolved organic matter. *Organic Geochemistry*, 152. https://doi.org/10.1016/j.orggeochem.2020.104141.

Pak, S. J. Moon, J. W. Kim, J. Chandler, M. T. Kim, H. S. Son, J. Son, S. K. Choi, S. K. and Baker, E. T. 2017. Widespread tectonic extension at the Central Indian Ridge between 8°S and 18°S. *Gondwana Research*, 45:163–179.

Plüger, W. L. Herzig, P. M. Becker, K. P. Deissmann, G. Schops, D. Lange, L. Jenisch, A. Ladage, S. Richnow, H. H. Schulz, T. and Michaelis, W. 1990. Discovery of hydrothermal fields at the Central Indian Ridge. *Marine Mining*, 9: 73–86.

Popoola, S. O. and Akintoye, A. E. 2021. Integrated geochemical investigations on Fe-Mn nodules, polymetallic sulfides and Fe-Mn oxides recovered from marine sediments of Carlsberg Ridge, Northwest Indian Ocean. *Advances in Environmental Studies*, 5(1): 394–403.

Popoola, S. O. Han, X. Wang, Y. Qiu, Z. Ye, Y. and Cai, Y. 2019. Mineralogical and geochemical signatures of metalliferous sediments in Wocan-1 and Wocan-2 hydrothermal sites on the Carlsberg Ridge, Indian Ocean. *Minerals*, 9(1): 26.

Qiu, Z. Han, X. G. Li, M. Wang, Y. Chen, X. Fan, W. Zhou, Y. Cui, R. and Wang, L. S. 2021. The temporal variability of hydrothermal activity of Wocan hydrothermal field, Carlsberg Ridge, northwest Indian Ocean. *Ore Geology Reviews*, 132: 103999.

Rajani, R. P. Banakar**,** V. K. Parthiban, G. Mudholkar, A. V. and Chodankar, A. R. 2005. Compositional variation and genesis of the ferromanganese crust of the Afanasiy-Nikitin Seamount, Equatorial Indian Ocean. *Journal of Earth System Sciences*, 114: 51–61.

Rajeevan, M. 2019. *Report of Blue Economy Working Group on National Accounting Framework and Ocean Governance*. Ministry of Earth Sciences, New Delhi India, p. 75 .

Ramana, M. V. Ramaprasad, T. Kamesh Raju, K. A. and Desa, M. 1993. Geophysical studies over a segment of the Carlsberg Ridge, Indian Ocean. *Marine Geology*, 115: 21–28.

Ray, D. Kamesh Raju, K. A. Baker, E. T. Srinivas Rao, A. Mudholkar, A. V. Lupton, J. E. Surya Prakash, L. Gawas, R. G. and Vijaya Kumar, T. 2012. Hydrothermal plumes over the Carlsberg Ridge, Indian Ocean. *Geochemistry, Geophysics, Geosystems*, 13(1).

Ray, D. Kamesh Raju, K. A. Srinivas Rao, A. Surya Prakash, L. Mudholkar, A. V. Yatheesh, V. Samudrakala, K. and Kota, D. 2020. Elevated turbidity and dissolved manganese in deep water column near 10° 47'S Central Indian Ridge: studies on hydrothermal activities. *Geo-Marine Letters*, 40: 619–628.

Ren, M. Chen, J. Shao, K. and Zhang, S. 2016. Metallogenic information extraction and quantitative prediction process of seafloor massive sulfide resources in the Southwest Indian Ocean. *Ore Geology Reviews*, 76: 108–121.

Scholten, J. C. Stoffers, P. Garbe-Schönberg, D. and Moammar, M. 2000. Hydrothermal mineralization in the Red Sea. In Cronan, D.S. (ed.), *Handbook of Marine Mineral Deposits*. CRC-Press, Boca-Raton, FL, pp. 369–395.

Scott, S. D. 1992. Olymetallic sulfide riches from the deep: Fact or fallacy? In Hsu, K.J. and Thiede, J. (eds), *Use and Misuse of the Seafloor*. New York, Wiley-Interscience, pp. 87–115.

Sun, C. Wu, Z. Tao, C. R. A. Zhang, G. Guo, Z. and Huang, E. 2018. The deep structure of the Duanqiao hydrothermal field at the Southwest Indian Ridge. *Acta Oceanologica Sinica*, 37: 73–79.

Swallow, J. C. and Crease, J. 1965. Hot salty water at the bottom of the Red Sea. *Nature*, 205: 165–166.

Tao, C. Li, H. Jin, X. Zhou, J. Wu, T. He, Y. Deng, X. Gu, C. Zhang, G. and Liu, W. 2014. Seafloor hydrothermal activity and polymetallic sulfide exploration on the southwest Indian Ridge. *Chinese Science Bulletin*, 59(19): 2266–2276.

Tao, C. Wu, G. Deng, X. Qui, Z. Han, C. and Long, Y. 2013. New discovery of seafloor hydrothermal activity on the Indian Ocean Carlsberg Ridge and Southern North Atlantic Ridge—progress during the 26th Chinese COMRA cruise. *Acta Oceanologica Sinica*, 32: 85–88. https://doi.org/10.1007/s13131–013–0345-x.

Tao, C. H. Li, H. M. Huang, W. Han, X. Q. Wu, G. H. Su, X. Zhou, N. Lin, J. He, Y. H. and Zhou, J. P. 2011. Mineralogical and geochemical features of sulfide chimneys from the 49° 39′ E hydrothermal field on the Southwest Indian Ridge and their geological inferences. *Chinese Science Bulletin*, 56(26): 2828–2838.

Tao, C. H. Lin, J. Guo, S. Q. Chen, Y. S. J. Wu, G. H. Han, X. Q. German, C. R. Yoerger, D. R. Zhou, N. Li, H. M. Su, X. and Zhu, J. 2012. First active hydrothermal vents on an ultraslow spreading center: Southwest Indian Ridge. *Geology*, 40(1): 47–50. doi: 10.1130/G32389.1.

Thaler, A. D. and Amon, D. 2019. 262 Voyages Beneath the Sea: a globalassessment of macro- and megafaunal biodiversity and research effort atdeep-sea hydrothermal vents. *PeerJ*, 7: e7397. doi: 10.7717/peerj.7397.

UN-DESA. World Population Prospects. 2019. Highlights. ST/ESA/SER.A/423. United Nations: New York, NY, USA.

Van Dover, C.L. 2000. *The Ecology of Deep-Sea Hydrothermal Vents*. Princeton University Press, Princeton, p. 412.

Van Dover, C. L. Arnaud-Haond, S. Gianni, M. Helmreich, S. Huber, J. A. Jaeckel, A. L. Metaxas, A. Pendleton, L. H. Petersen, S. Ramirez-Llodra, E. Steinberg, P. E. Tunnicliffe, V. and Yamamoto, H. 2018. Scientific rationale and international obligations for protection of active hydrothermal vent ecosystems from deep-sea mining. *Marine Policy*, 90: 20–28. doi: 10.1016/j.marpol.2018.01.020.

Van Dover, C. L. Humphris, S. E. Fornari, D. Cavanaugh, C. M. Collier, R. Goffredi, S. K. Hashimoto, J. Lilley, M. D. Reysenbach, A. L. Shank, T. M. Von Damm, K. L. Banta, A. Gallant, R. M. Götz D. Green, D. Hall, J. Harmer, T. L. Hurtado, L. A. Johnson, P. McKiness, Z. P. Meredith, C. Olson, E. Pan, I. L. Turnipseed, M. Won,Y. Young III, C. R. and Vrijenhoek, R.C. 2001. Biogeography and ecological setting of Indian Ocean hydrothermal vents. *Science*, 294(5543): 818–823. doi: 10.1126/science.1064574.

Veizer, J. Laznicka, P. and Jansen, S. L. 1989. Mineralization through geologic time: recycling perspective. *American Journal of Science*, 289(4): 484–524. doi: https://doi.org/10.2475/ajs.289.4.484.

Wang, S. Sun, W. Huang, J. and Zhai, S. 2021. Iron and sulfur isotopes of sulfides from the Wocan hydrothermal field, on the Carlsberg Ridge, Indian Ocean. *Ore Geology Reviews*, 103971.

Wang, Y. Han, X. Petersen, S. Frische, M. Qiu, Z. Li, H. Wu, R. and Cui, R. 2017. Mineralogy and trace element geochemistry of sulfide minerals from the Wocan Hydrothermal Field on the slow-spreading Carlsberg Ridge, Indian Ocean. *Ore Geology Reviews*, 84: 1–19.

Wang, Y. Han, X. Zhou, Y. Qiu, Z. Yu, X. Petersen, S. Li, H. Yang, M. Chen, Y. Liu, J. Wu, X. and Luo, H. 2020. The Daxi Vent Field: an active mafic-hosted hydrothermal system at a non-transform offset on the slow-spreading Carlsberg Ridge, 6°48′N. *Ore Geology Reviews*, 103888. doi: 10.1016/j.oregeorev.2020.1038.

Wang, Y. Wu, Z. Sun, X. Deng, X. Guan, Y. Xu, L. Huang, Y. and Cao, K. 2018. He–Ar–S isotopic compositions of polymetallic sulfides from hydrothermal vent fields along the ultraslow-spreading Southwest Indian Ridge and their geological implications. *Minerals*, 8(11): 512.

Wilson, D. S. 1993. Confidence intervals for motion and deformation of the Juan de Fuca plate. *Journal of Geophysical Research*, 98: 16053–16071.

Wu, Z. Sun, X. Xu, H. Konishi, H. Wang, Y. Lu, Y. Cao, K. Wang, C. and Zhou, H. 2018. Microstructural characterization and in-situ sulfur isotopic analysis of silver-bearing sphalerite from the Edmond hydrothermal field, Central Indian Ridge. *Ore Geology Reviews*, 92: 318–347.

Yang, W. Tao, C. Shili, L. Liang, J. Liu, J. and Li, W. 2019. Geological fate of seafloor polymetallic sulfides at the Duanqiao hydrothermal field (Southwest Indian Ridge). In *AGU Fall Meeting Abstracts* (Vol. 2019, pp. OS33C-1821).

Yang, W. Tao, C. Li, H. Liang, J. Liao, S. Long, J. Ma, Z. and Wang, L. 2017. 230Th/238U dating of hydrothermal sulfides from Duanqiao hydrothermal field, Southwest Indian Ridge. *Marine Geophyshysical Research*, 38: 71–83. https://doi.org/10.1007/s11001–016–9279-y.

Yi, S. B. Lee, M. J. Park, S. H. Nagao, K. Han, S. Yang, S. Y. Choi, H. Baek, J. and Sumino, H. 2021. Alkalic to tholeiitic magmatism near a mid-ocean ridge: petrogenesis of the KR1 Seamount Trail adjacent to the Australian-Antarctic Ridge. *International Geology Review*, 63(10): 1215–1235, doi: 10.1080/00206814.2020.1756002.

Yu, J. Tao, C. Liao, S. Alveirinho Dias, A. Liang, J. Yang, W. and Zhu, C. 2021. Resource estimation of the sulfide-rich deposits of the Yuhuang-1 hydrothermal field on the ultraslow-spreading Southwest Indian Ridge. *Ore Geology Reviews*. doi: https://doi.org/10.1016/j.oregeorev.2021.104169.

Yu, Z. Li, H. Li, M. and Zhai, S. 2018. Hydrothermal signature in the axial-sediments from the Carlsberg Ridge in the northwest Indian Ocean. *Journal of Marine Systems*, 180: 173–181.

Yue, X. Li, H. Ren, J. Tao, C. Zhou, J. Wang, Y. and Lü, X. 2019. Seafloor hydrothermal activity along mid-ocean ridge with strong melt supply: study from segment 27, southwest Indian ridge. *Scientific Reports*, 9(1): 1–10.

Zhou, Y. Zhang, D. Zhang, R. Liu, Z. Tao, C. Lu, B. Sun, D. Xu, P. Lin, R. Wang, J. and Wang, C. 2018. Characterization of vent fauna at three hydrothermal vent fields on the Southwest Indian Ridge: implications for biogeography and interannual dynamics on ultraslow-spreading ridges. *Deep Sea Res Part I: Oceanographic Research Papers*, 137: 1–12. doi: 10.1016/j.dsr.2018.05.0018.

Zhu, C. Tao, C. Yin, R. Liao, S. Yang, W. Liu, J. and Barriga, F.J. 2020. Seawater versus mantle sources of mercury in sulfide-rich seafloor hydrothermal systems, Southwest Indian Ridge. *Geochimica et Cosmochimica Acta*, 281: 91–101.